PCCP

COMMUNICATION

View Article Online
View Journal | View Issue

Cite this: *Phys. Chem. Chem. Phys.*, 2014, **16**, 895

Received 24th September 2013,
Accepted 13th November 2013

DOI: 10.1039/c3cp54036g

www.rsc.org/pccp

Particle size dependence on oxygen reduction reaction activity of electrodeposited TaO_x catalysts in acidic media

Jeongsuk Seo,[a] Dongkyu Cha,[b] Kazuhiro Takanabe,[c] Jun Kubota[ad] and Kazunari Domen*[a]

The size dependence of the oxygen reduction reaction activity was studied for TaO_x nanoparticles electrodeposited on carbon black for application to polymer electrolyte fuel cells (PEFCs). Compared with a commercial Ta_2O_5 material, the ultrafine oxide nanoparticles exhibited a distinctively high onset potential different from that of the bulky oxide particles.

In the past few decades, there have been many attempts to replace Pt or Pt-based electrocatalysts with new non-precious materials applicable in polymer electrolyte fuel cells (PEFCs). In particular, various promising non-platinum candidates have been reported as oxygen reduction reaction (ORR) electrocatalysts with a high activity comparable to those of commercial Pt/C catalysts, such as N-coordinated Fe- and Co-based catalysts, and N-doped metal-free carbon-based catalysts.[1–5] However, their superior catalytic activities for the ORR are not applicable to PEFCs, because the transition metal-based and N-doped catalysts are chemically unstable in acidic media, which means that their high activity cannot be maintained in long-term PEFC operation. Hence, based on their high durability in acidic atmospheres, several Ta-, Nb-, and Zr-based catalysts of groups IV and V have been researched as ORR electrocatalysts.[6–15] Despite their high stability, their extremely poor electroconductivity resulted in a low activity for the ORR. Many approaches to overcome this limitation were investigated, such as nitride or partially oxynitride compounds achieved by doping with N or by varied heat treatments.[6–8,10,12,16] Unfortunately, the improved activity has repeatedly resulted in no long-term performance benefit because these materials tend to oxidize under acidic PEFC conditions. In fact, oxides are commonly known as the most stable substances in acidic media.[17] Pure group IV or V metal oxides without C or N doping are generally insulators in bulk structures. As a result, most bulk oxide catalysts have shown a very low current density for the ORR, even with a high onset potential.[3,15–17]

It is very difficult to control group IV or V oxides on the nanoscale using conventional methods such as impregnation. Primary particles of oxide catalysts smaller than 10 nm can be prepared, but these fine particles easily aggregate to form larger secondary particles during high-temperature preparation. We recently reported group IV and V oxide nanoparticles of TaO_x, NbO_x, and ZrO_x supported on carbon black (CB) prepared by potentiostatic electrodeposition as ORR electrocatalysts.[11,13,18] Electrodeposition has been used to control the size and distribution of metal particles on conductive substrates in various fields.[19–21] Group IV and V metal precursors are not soluble in aqueous solutions because of precipitation reactions with H_2O to form oxides or hydroxides. Thus, the electrodeposition of metal species was first attempted in non-aqueous metal ethoxide solutions at room temperature, and oxide nanoparticles were successfully deposited uniformly on CB. The ultrafine oxide nanoparticles without any doping showed excellent ORR activity, with a high onset potential that should not have occurred in bulky particles. The high current retention of the TaO_x catalysts in the ORR after a long-term stability test in an aqueous sulfuric solution further supported the high stability of these oxide materials in acidic media.[13]

Group IV and V oxide nanoparticles formed by electrodeposition exhibited very different electrocatalytic behavior from that of common bulky oxide particles. The relationship between oxide nanoparticle size and electrocatalytic performance is not yet fully understood. Also, the effect of particle size on ORR activity requires a new perspective on group IV and V oxide nanoparticles. For metallic catalysts such as Pt, the increase in electrochemical surface area (ECSA) resulting from size reduction has typically been cited as the reason for improved electrocatalytic activity. However, for group IV and V oxide nanoparticles, the enhanced

[a] *Department of Chemical System Engineering, The University of Tokyo, 7-3-1 Hongo, Bunkyo-ku, Tokyo 113-8656, Japan. E-mail: domen@chemsys.t.u-tokyo.ac.jp*
[b] *Advanced Nanofabrication, Imaging and Characterization Laboratory, King Abdullah University of Science and Technology (KAUST), Thuwal 23955-6900, Saudi Arabia*
[c] *Division of Chemical and Life Sciences and Engineering, KAUST Catalysis Center (KCC), King Abdullah University of Science and Technology (KAUST), 4700 KAUST, Thuwal 23955-6900, Saudi Arabia*
[d] *Elements Strategy Initiative for Catalysts and Batteries (ESICB), Kyoto University, Katsura, Kyoto 615-8520, Japan*

ORR activity resulting from size reduction should be attributed to increased electroconductivity and an increased number of active sites on the catalyst surface. In this study, we successfully prepared TaO_x nanoparticles of different sizes by electrodeposition. The particle size of the deposited species was determined by varying deposition parameters such as the applied potential or deposition time, and/or by altering the deposition environment by changing the concentration of the primary precursor or electrolyte or by adjusting the deposition temperature. The particle size dependence of the ORR electrocatalytic activity of electrodeposited TaO_x nanoparticles will be discussed. Furthermore, a critical factor controlling the particle size of oxide catalysts will be introduced after comparing various deposition conditions.

For the preparation of TaO_x electrocatalysts, bare CB electrodes as conductive substrates for electrodeposition were first prepared using a CB powder with an average size of 30–40 nm (Vulcan-XC72). The CB powder was mixed with a Nafion ionomer solution (Aldrich 1100EW, 5 wt% in water–aliphatic alcohols) and isopropyl alcohol (IPA, 99.9%, Kanto Chemical). The composition ratio of the CB powder to the ionomer solution was fixed at 2 : 3 by weight. The CB slurry was stirred and sonicated repeatedly to achieve good dispersion. Subsequently, the highly dispersed CB slurry was sprayed onto carbon paper (EC-TP1-060T, Toyo Corporation, treated with polytetrafluoroethylene (PTFE)) at 343 K with a CB loading of 0.5 mg cm^{-2}. The sprayed bare CB electrodes were completely dried at 343 K.

Potentiostatic electrodeposition of Ta species onto the bare CB electrode was performed in a three-electrode system using a potentiostat (HZ5000, Hokuto Denko). The bare CB electrode with an area of 1 cm^2 was mounted as a working electrode. A carbon rod and an Ag/AgCl electrode (HX-R4, Hokuto Denko) were used as counter and reference electrodes, respectively. The carbon rod was selected to avoid Pt contamination. The three electrodes were immersed in a $TaCl_5$ (Wako Chemicals) or a $Ta(OC_2H_5)_5$ (99.9%, Wako Chemicals) ethanol solution with a supporting electrolyte of $NaClO_4$ (99%, Sigma-Aldrich) at 298 K. Constant potentials were applied to the bare CB electrode for 10 s. After the electrodeposition, the electrodes were sufficiently washed by ethanol to remove the metal precursor residues, and completely dried at 298 K. Finally, the as-electrodeposited electrodes were heated under pure H_2 flow at 523 K for 30 min at a ramp rate of 5 K min^{-1} to modify their surface. The effects of the H_2 treatment on the ORR activity were discussed in our previous papers.[11,13] The detailed conditions of electrodeposition are summarized in Table 1, with the resulting loading amount of Ta estimated using inductively coupled plasma-atomic emission spectrometry (ICP-AES).

Fig. 1 shows transmission electron microscope (TEM) and scanning TEM (STEM) images of TaO_x electrocatalysts. The dark and bright circles in the TEM and STEM images, respectively, are TaO_x particles electrodeposited on CB particles 30–40 nm in diameter. The TaO_x particles seem to have different sizes in different samples. The diameters of several tens of nanoparticles were obtained for each sample from several TEM and STEM images, with the results shown in the histograms of Fig. 1. The average particle diameters and the standard deviations are shown in Table 1. The particle size increased monotonically from (a) to (d). Briefly, the $TaCl_5$ precursor resulted in the formation of smaller particles compared to $Ta(OEt)_5$,

Table 1 Electrodeposition conditions for different sizes of TaO_x catalysts, along with their loading amounts and particle sizes. All depositions were performed in 20 mM Ta plating baths. $NaClO_4$ was used as an electrolyte. The amounts of electrodeposited Ta were determined by ICP-AES. The particle sizes were averaged over the TaO_x nanoparticles above 50 spots, respectively

Sample	Ta precursor	$NaClO_4$ (mM)	Potential ($V_{Ag/AgCl}$)	Loading (mg-Ta cm^{-2})	Average size[a] (nm)
a	$TaCl_5$	20	−0.5	0.016	1.0 ± 0.3
b	$TaCl_5$	20	−0.3	0.013	2.6 ± 0.9
c	$TaCl_5$	50	−0.5	0.023	4.6 ± 0.7
d	$Ta(OEt)_5$	20	−0.5	0.034	13.5 ± 3.3

[a] The standard deviation of 1σ is indicated as an error.

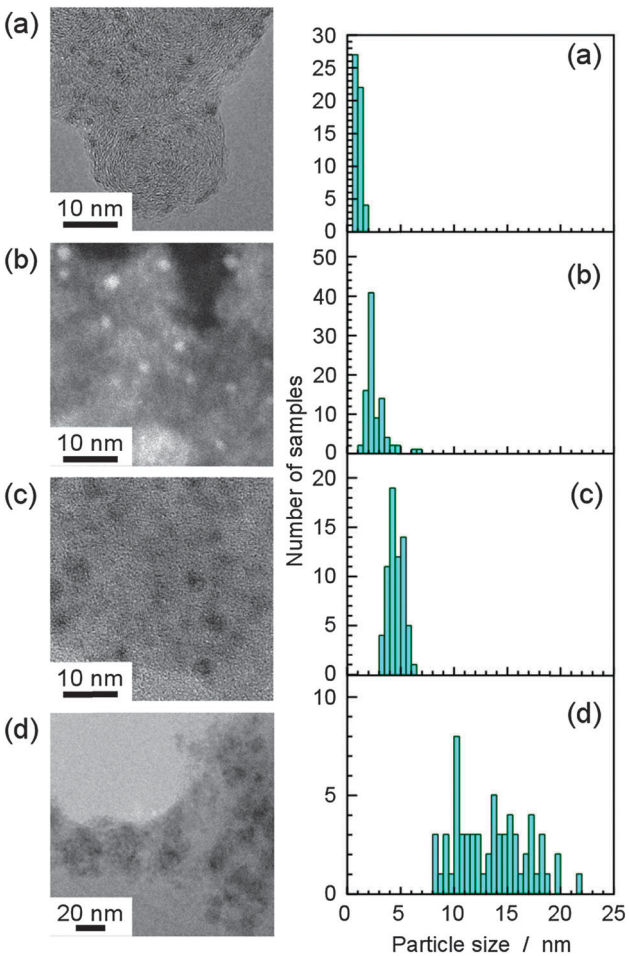

Fig. 1 TEM (a, c, d) and STEM (b) images and the particle size distribution of differently sized TaO_x catalysts. (a)–(d) correspond to samples (a)–(d) in Table 1.

and the higher concentration of the supporting electrolyte caused the formation of larger TaO_x particles under the same deposition parameters, applied potential and deposition time. At a positive potential of −0.3 $V_{Ag/AgCl}$, larger particles were deposited on CB than at −0.5 $V_{Ag/AgCl}$. The electrodeposition of TaO_x in a $TaCl_5$ ethanol solution is accompanied by H_2 evolution from the HCl formed from $TaCl_5$ and ethanol.[13] This side reaction probably affects the formation of smaller TaO_x particles. In any case, TaO_x nanoparticles of different sizes were successfully electrodeposited on CB electrodes under different applied potentials

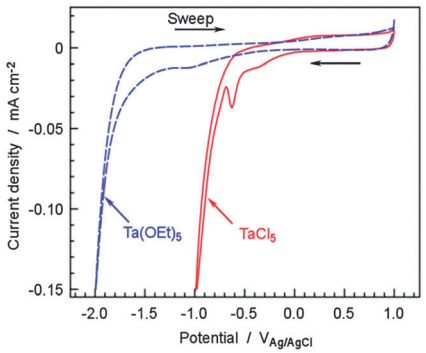

Fig. 2 Cyclic voltammograms of Ta species on glassy carbon (GC) in non-aqueous solutions of $TaCl_5$ in ethanol (solid red line) and a dilution of liquid $Ta(OEt)_5$ in ethanol (dashed blue line) under Ar purging at 298 K. 20 mM $NaClO_4$ was dissolved in the solutions as a supporting electrolyte. The potential was cycled over the range from −2 or −1 to 1 $V_{Ag/AgCl}$ at a scan rate of 5 mV s^{-1}.

and Ta plating baths. Although the detailed mechanism of electrodeposition has not been clear yet, the Ta species were considered to be reductively deposited on the CB surfaces with chemical adsorption and they were re-oxidized right after the exposure to air. Because the electrodeposition of Ta took place with H_2 evolution, the Faradaic efficiency for the electrodeposition was about 60% for sample (a).

Cyclic voltammograms (CVs) of glassy carbon (GC) electrodes in 20 mM $TaCl_5$ and 20 mM $Ta(OEt)_5$ ethanol solutions are shown in Fig. 2. As reported in our previous paper,[13] for the $TaCl_5$ solution, the shoulder peaks around −0.5 $V_{Ag/AgCl}$ represent the reduction of Ta^{5+} to Ta^{4+} and Ta^{3+}, resulting in the deposition of Ta-containing species on the CB. The high cathodic current at approximately −1.0 $V_{Ag/AgCl}$ was mainly due to H_2 evolution from the HCl byproduct. In the $Ta(OEt)_5$ solution, there was no significant cathodic current at around −1.0 $V_{Ag/AgCl}$, indicating that H_2 evolution from the HCl byproduct did not occur in this solution. The shoulder peaks corresponding to the reduction of Ta^{5+} were broad and unclear for the $Ta(OEt)_5$ solution. This difference in electrochemical properties between $TaCl_5$ and $Ta(OEt)_5$ ethanol solutions resulted in different TaO_x particle sizes.

The ORR properties of TaO_x electrocatalysts with various sizes in a 0.1 M H_2SO_4 solution were investigated, as shown in Fig. 3A. The measurements were carried out in a conventional single-vessel electrochemical cell with Ag/AgCl reference and carbon counter electrodes. The potential of 1.23 to 0.20 V_{RHE} was linearly scanned in the cathodic direction with a scan rate of 5 mV s^{-1} at 298 K, and the current difference between O_2- and Ar-purged atmospheres is shown in the vertical axis. Because of the difficulty of fabrication of the rotating disk electrode (RDE) using our electrocatalysts, we cannot evaluate kinetic current for ORR and the ORR properties of the catalysts on a carbon sheet were compared. The ORR results for a Ta metal plate (99.95%, Nilaco), the Ta_2O_5 powder sprayed on a bare CB electrode with a loading of 0.25 mg cm^{-2} (99.9%, 500 nm particle size, High Purity Chemicals), and a bare CB electrode are also shown in Fig. 3A. The electrodeposited TaO_x electrocatalysts with particle sizes below 4.6 nm showed significant ORR currents, with onset

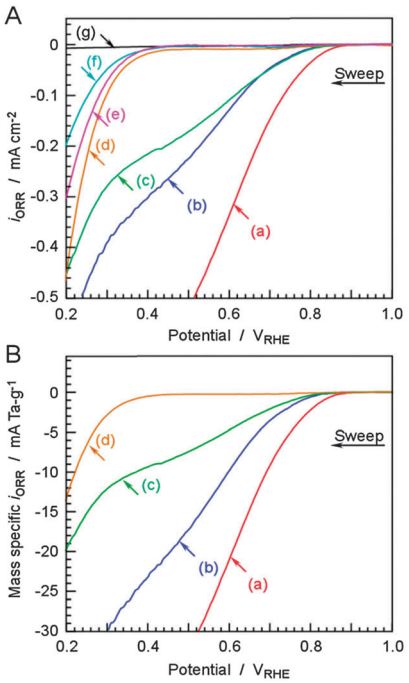

Fig. 3 (A) Linear sweep voltammograms of differently sized TaO_x nanoparticles deposited on CB electrodes in an average of 1.0 (a), 2.6 (b), 4.6 (c), and 13.5 (d) nm. The ORRs on the electrodeposited TaO_x catalysts were compared with those on a bare CB electrode (as a blank, (e)), commercial Ta_2O_5 particles (500 nm, (f)), and a Ta metal plate (g). The potential was cathodically swept in the 0.1 M H_2SO_4 aqueous solution at a scan rate of 5 mV s^{-1} at 298 K. The current i_{ORR} indicates the difference in current density between Ar- and O_2-saturated atmospheres. (B) Linear sweep voltammograms from (A) converted to a mass-specific current density.

potentials of 0.8–0.92 V_{RHE}. The TaO_x electrocatalyst with a particle size of 13.5 nm exhibits similar ORR activity to those of CB and the Ta_2O_5 powder. The Ta metal plate was covered with a thick passivation layer, so a negligible ORR current was expected. Voltammograms corrected to mass-specific ORR currents are also shown in Fig. 3B. The ORR activities clearly decreased with increasing particle size, up to 13.5 nm.

Mass-specific ORR currents at 0.6 V_{RHE} and onset potentials at 2 μA cm^{-2} are plotted in Fig. 4. The negative shift in onset potential with increasing particle size was only 0.13 V, however, the current density decreased drastically. The current density fell to nearly zero for the largest TaO_x nanoparticles, which were 13.5 nm in size, indicating that these particles are not useful electrocatalysts. The mass activities on the TaO_x electrodes increased significantly as their size decreased. The electrochemical relationship between the particle size of metallic catalysts such as Pt or Pd and their activity has been generally discussed in an ECSA.[22–24] In fact, to date, it has been difficult to determine the practical ECSA of non-platinum catalysts because of a lack of technical methods such as measuring the adsorption–desorption peak of H^+ on the surface of a Pt catalyst. A more specific discussion of the ECSA was therefore unrealizable for the TaO_x catalysts of different sizes. The density of molecularly adsorbed oxygen on TiN nanoparticles is known to depend on the particle size.[12] This indicates that the number of active sites is not proportional to the geometric surface area of

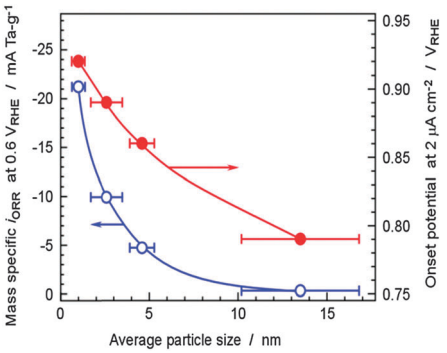

Fig. 4 Dependence of the mass specific current at 0.6 V_{RHE} and onset potential at 2 μA cm^{-2} on the average size of TaO_x nanoparticles electrodeposited on CB. The error bars indicate the standard deviation of 1σ for each particle size.

particles, and that we should consider the increased active site density per unit area with decreasing particle size. However, for TaO_x electrocatalysts, the influence of the ultrafine particle size on the high activity is attributed to the increase of the electroconductivity of the particles different from the bulky oxides and the increase in the density of electrochemical active sites. Macagno *et al.* have reported that the donor density for a ferroelectric layer of the Ta_2O_5 film decreases with increasing thickness, and films thicker than 10 nm behave as pure insulators.[25] In this work, the ORR current increased drastically for TaO_x electrocatalysts smaller than 4.6 nm, indicating that the particle size is the most important factor determining the ORR activity of the oxide electrocatalysts.

Conclusions

In summary, we introduced a new approach to determine the size dependence of the ORR activity of TaO_x nanoparticles for use as electrocatalysts in PEFCs. TaO_x nanoparticles of different sizes were successfully prepared by electrodeposition in non-aqueous $TaCl_5$ or $Ta(OEt)_5$ ethanol solutions at 298 K by varying deposition conditions such as the applied potential or the concentration of the plating bath. The electrodeposited TaO_x nanoparticles exhibited size-dependent electrocatalytic performance, *i.e.* the smallest oxide particles have the highest ORR activity due to their improved electroconductivity and an increase of electrochemically active sites. Consequently, based on their high chemical stability under acidic conditions, these highly active oxide nanoparticles are proposed as potential non-platinum electrocatalysts for PEFC cathodes.

This work was supported in part by the Funding Program for World-Leading Innovative R&D on Science and Technology (FIRST) of the Cabinet Office of Japan, the International Exchange Program of the A3 Foresight Program of the Japan Society for the Promotion of Science (JSPS), and the ''Elements Strategy Initiative to Form Core Research Center'' (since 2012) of the Ministry of Education, Culture, Sports, Science and Technology (MEXT), Japan.

Notes and references

1 M. Lefevre, E. Proietti, F. Jaouen and J. P. Dodelet, *Science*, 2009, **324**, 71.
2 G. Wu, K. L. More, C. M. Johnston and P. Zelenay, *Science*, 2011, **332**, 443.
3 H. T. Chung, J. H. Won and P. Zelenay, *Nat. Commun.*, 2013, **4**, 1922.
4 K. Gong, F. Du, Z. Xia, M. Durstock and L. Dai, *Science*, 2009, **323**, 760.
5 L. T. Qu, Y. Liu, J. B. Baek and L. M. Dai, *ACS Nano*, 2010, **4**, 1321.
6 A. Ishihara, S. Doi, S. Mitsushima and K.-I. Ota, *Electrochim. Acta*, 2008, **53**, 5442.
7 A. Ishihara, Y. Ohgi, K. Matsuzawa, S. Mitsushima and K.-I. Ota, *Electrochim. Acta*, 2010, **55**, 8005.
8 Y. Ohgi, A. Ishihara, K. Matsuzawa, S. Mitsushima and K. Ota, *J. Electrochem. Soc.*, 2010, **157**, B885.
9 F. Yin, K. Takanabe, M. Katayama, J. Kubota and K. Domen, *Electrochem. Commun.*, 2010, **12**, 1177.
10 S. Isogai, R. Ohnishi, M. Katayama, J. Kubota, D. Y. Kim, S. Noda, D. Cha, K. Takanabe and K. Domen, *Chem.–Asian J.*, 2012, **7**, 286.
11 J. Seo, D. Cha, K. Takanabe, J. Kubota and K. Domen, *Chem. Commun.*, 2012, **48**, 9074.
12 R. Ohnishi, K. Takanabe, M. Katayama, J. Kubota and K. Domen, *J. Phys. Chem. C*, 2013, **117**, 496.
13 J. Seo, L. Zhao, D. Cha, K. Takanabe, M. Katayama, J. Kubota and K. Domen, *J. Phys. Chem. C*, 2013, **117**, 11635.
14 T. Oh, J. Y. Kim, Y. Shin, M. Engelhard and K. S. Weil, *J. Power Sources*, 2011, **196**, 6099.
15 J. Y. Kim, T.-K. Oh, Y. Shin, J. Bonnett and K. S. Weil, *Int. J. Hydrogen Energy*, 2011, **36**, 4557.
16 Y. Liu, A. Ishihara, S. Mitsushima, N. Kamiya and K.-I. Ota, *Electrochem. Solid-State Lett.*, 2005, **8**, A400.
17 A. Rabis, P. Rodriguez and T. J. Schmidt, *ACS Catal.*, 2012, **2**, 864.
18 J. Seo, D. Cha, K. Takanabe, J. Kubota and K. Domen, *ACS Catal.*, 2013, **3**, 2181.
19 S. Zein El Abedin, U. Welz-Biermann and F. Endres, *Electrochem. Commun.*, 2005, **7**, 941.
20 W. Simka, D. Puszczyk and G. Nawrat, *Electrochim. Acta*, 2009, **54**, 5307.
21 J. Lee, J. Seo, K. Han and H. Kim, *J. Power Sources*, 2006, **163**, 349.
22 M. Nesselberger, S. Ashton, J. C. Meier, I. Katsounaros, K. J. Mayrhofer and M. Arenz, *J. Am. Chem. Soc.*, 2011, **133**, 17428.
23 M. Shao, A. Peles and K. Shoemaker, *Nano Lett.*, 2011, **11**, 3714.
24 W. Tang, H. Lin, A. Kleiman-Shwarsctein, G. D. Stucky and E. W. McFarland, *J. Phys. Chem. C*, 2008, **112**, 10515.
25 V. A. Macagno and J. W. Shchultze, *J. Electroanal. Chem.*, 1984, **180**, 157.